Acta Dermatovener (Stockholm) 54: 161–172, 1974

ULTRASTRUCTURE OF FREEZE-CLEAVED STRATUM BASALE AND STRATUM MALPIGHII

Ken Hashimoto

From the Veterans Administration Hospital, Memphis, Tennessee and the Department of Anatomy and Division of Dermatology, the University of Tennessee College of Medicine, Memphis, Tennessee, USA

Abstract. The basal and Malpighian layers of the human epidermis were freeze-cleaved in a high vacuum and the cleaved surfaces were replicated with platinum and carbon. Examination of the replicas showed tonofibrils in various patterns of organization and two distinctly different fractured surfaces of plasma membranes. The A-face at a nexus was characterized by patches of aggregated small particles (100–135 Å) and scattered membrane-associated particles, which were never as abundant as shown in other tissue or cells. The B-face at a nexus showed aggregation of cobblestone-like low particles. Pits were occasionally seen on the B surface but not as commonly as described in other organs. Membrane-associated particles were only sparsely distributed on the B surface.

Except for the studies done on the human cervical epithelium by McNutt & Weinstein (9) and McNutt, Hershberg & Weinstein (10), there are no quotable works in the literature on the human keratinizing epithelia as examined by the method of freeze-cleavage or freeze-etching. The major contribution so far made with this technique seems to be the analysis of membrane structure and cell-to-cell junctions at the ultrastructural level.

In this study, *en face* views of keratinocyte membrane and nexus (gap junction) were examined. In agreement with the observations made by McNutt & Weinstein (9) and McNutt et al. (10) in the normal cervical epithelia and with the findings of other investigators on red blood cells (12, 15), liver cells (4), and on an experimental model of the cell membrane (3), the cleaved surfaces of many keratinocytes were found to be either face A or face B (see below). This report deals with the surface structures of the freeze-cleaved cytomembranes and nexuses of the human epidermis and their correlation with the images observed in thin sections with the aid of lanthanum.

METHODS AND MATERIALS

Normal skin specimens were obtained from the face, arm, hand, leg, and foot of several adults by 2–4 mm punches under local anesthesia with 1% procaine. In addition, thick epidermis from the lateral aspect of a right ring finger was removed when a friction blister was developed by a screwdriver. Some specimens were sliced and immediately frozen in liquid nitrogen at −170°C. Other specimens were fixed for several hours in 5% glutaraldehyde in 1/10 cacodylate buffer, pH 7.4, rinsed in the same buffer overnight and then processed in the same way as non-fixed tissue. A Denton DFE-2 freeze-etch apparatus attached to a DV-502 evaporator was used throughout. Apposed specimen holders were used to mount the specimens. Specimens were fractured at between −170°C and −200°C and shadowed at a 45° angle with a mixture of platinum and carbon and then coated with carbon at between −120°C and −100°C. The fracture surfaces were either etched by sublimation in vacuum ($10^{-6} \times 6$ torr) or not, prior to shadowing. The replicas thus produced were detached from the tissue with 30% Clorox and cleaned in three changes of distilled water. The cleaned replicas were placed on 200-mesh copper grids coated with Formvar and examined in a Hitachi HU-12 electron microscope operated at 125 kV. A part of the epidermal roof of the friction blister was permeated with lanthanum after a brief fixation in 2% glutaraldehyde to which 1% lanthanum nitrate was added. Parts of the other skin specimens were permeated with 1% colloidal lanthanum hydroxide. The details of these methods have been reported previously (5, 6, 7) as a modification of the Revel and Karnowsky technique (13).

Interpretation of freeze-cleaved membrane surface

The plane of the membrane cleavage by freeze-fracture procedures has been controversial: (i) the cleavage plane goes over the real cell surface; (ii) the membrane is split in the interior through a lipid bilayer (1, 12) and thus two new faces are created (9, 10); (iii) both real membrane surface and split membrane surfaces are revealed (14); and (iv) the position is undecided. Cell surface labelling with ferritin failed to demonstrate the ferritin particles on the cleaved surface (12). The real cell surface of erythrocytes as revealed by sublimation of water in which they were embedded is smooth, whereas the fractured surfaces are studded with small particles,

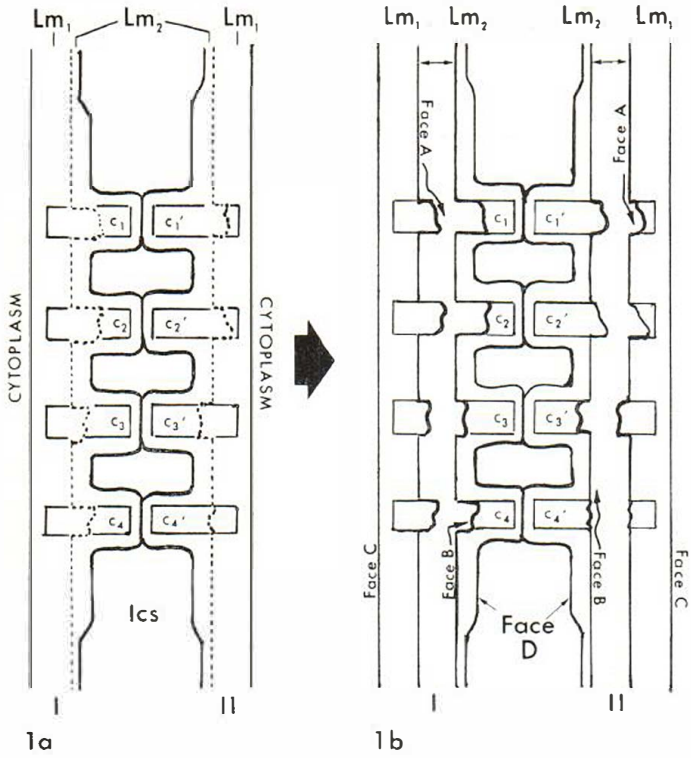

Fig. 1. (*a*) Cell membranes of two apposed keratinocytes (*I, II*) are separated by the intercellular space (*Ics*). In the nexus the outer surfaces of two membranes are fused intermittently by projected subunits that cover the contact cylinders (C_1, C_1', C_2, C_2', C_3, C_3', C_4, C_4'). Broken lines indicate the potential cleavage planes which will split the membranes into Lm1 and Lm2 (cf. Fig. 1*b*). In membrane I, contact cylinders are broken at various levels within Lm2 and, when Lm1 and Lm2 are separated, project out as A-face particles (cf. Fig. 1*b*). Although not shown, a more conventional pattern of cleavage may occur: Contact cylinders are pulled out completely from Lm2, giving rise to very high A-face particles. In membrane II, contact cylinders are fractured within Lm1 (C_1', C_2'), within Lm2 (C_3') or level with the cleavage plane (C_4'). (*b*) The cleavage of the membranes I and II creates Face A and Face B. Extracellular surface is designated Face D and juxtacytoplasmic surface, Face C. The split membrane I exposes fractured contact cylinders as A-face particles, all of which are projected out of Face A, and as pits all indented into Face B: thus, classic Face A particles and Face B pits are produced. The fracture of membrane II reveals on Face B low profiles of fractured cylinders, namely cobblestone particles (C_1', C_2'), slightly depressed pits (C_3') and the area level with the cleavage plane (C_4'). This combination actually occurs in some fractured membranes (inset of Fig. 4). Since the counterpart of this type of fracture shows a similar variety of broken cylinders (Face A of II), it may be difficult to distinguish Face A from Face B.

i.e., the membrane-associated particles (MAP) (12, 15). The double replica technique produced two distinctly different sets of membrane faces that are complementary (2), instead of producing a set of smooth and symmetrical surfaces which one might have expected if the intact cell surfaces of two apposed cells were revealed (11). Although this problem does not seem to have been settled completely, the membrane-splitting hypothesis of Branton (1) as supported by McNutt & Weinstein (9), Chalcroft & Bullivant (2) and others (10, 12, 15) will be adopted and the terminology developed by this group will be followed. According to their assumption, when the intact membrane is split, the cytoplasmic or inner lamella (Lm1) gives outwardly directed "face A". The true cell surface, i.e., "face D" is said not to be revealed at the nexus and the juxtacytoplasmic surface, i.e., "face C", can be seen

Fig. 2. Malpighian cells of the normal skin of the hand. Bundles of tonofibrils (*T*) are seen in various patterns. Fractured cytomembranes are revealed in cross section as well as in face view. An A-face (A) shows more MAPs than a B-face (B). The nexus on the A-face (*) has an aggregation of high particles, i.e., contact cylinders, whereas the nexus on the B-face (**) shows a slight depression and pits or cobblestone pattern. The ill-defined area (D) between two nexuses on the B-face is studded with small particles and might correspond to a desmosomal area. (*Arrow*) direction of platinum casting: in the following illustrations large arrows always indicate the same. *v*, cytoplasmic vesicles. × 175 000.

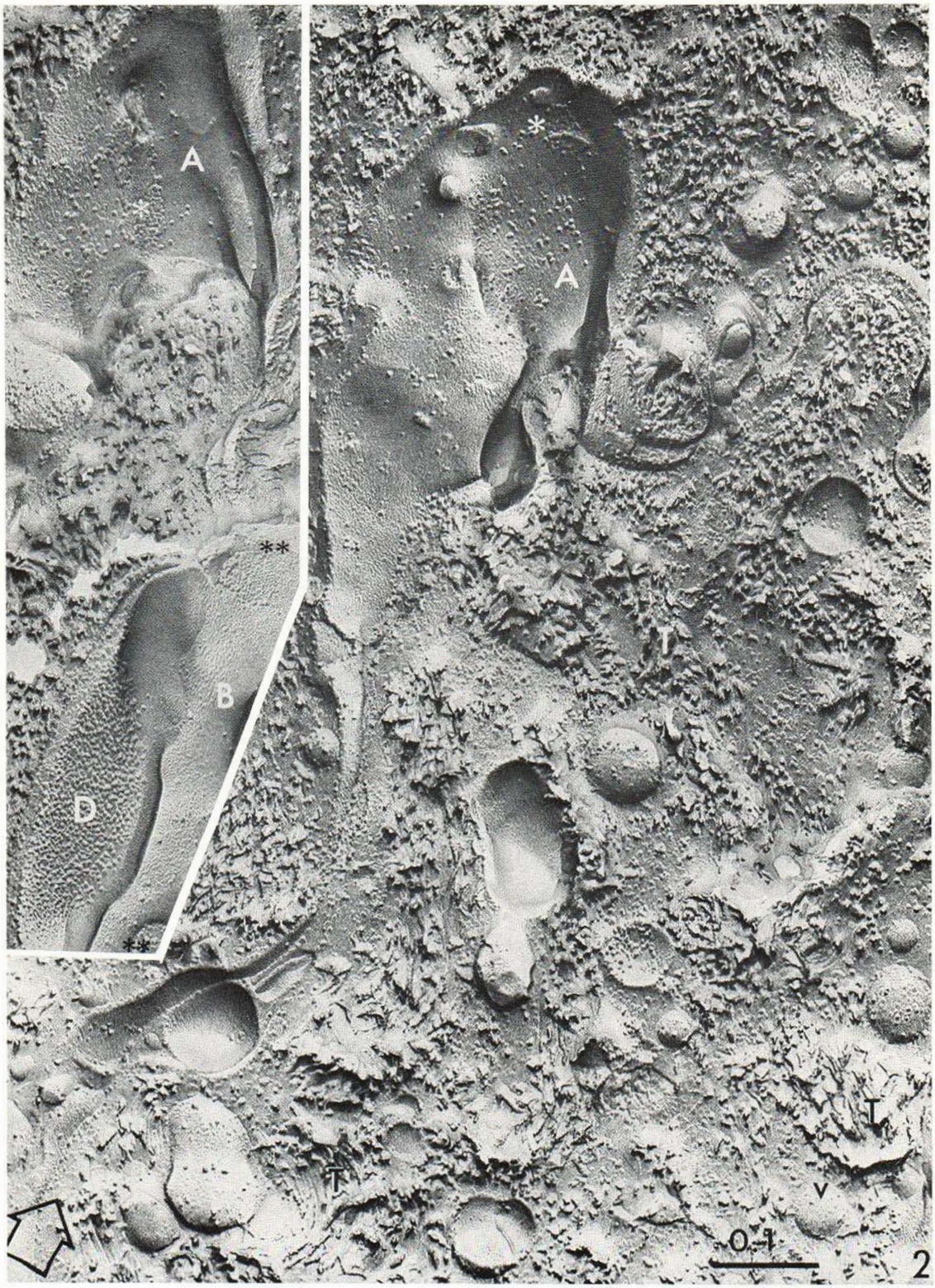
A
*
**
B
D
**
A
*
T
T
T
V
0.1
2

only after intensive etching of the cytoplasmic substance covering this surface (9) (Fig. 1*b*).

RESULTS

General description

Membranes, cytoplasm, and various organelles were replicated (Fig. 2). Bundles of tonofibrils were seen projecting out of the cleavage plane, particularly in those specimens etched slightly by sublimation (Fig. 2). An embossed fibrillar pattern of tonofibrils in parallel, weaving or whorl formation could be visualized (Fig. 2). The fracture surfaces of small as well as large vesicles showed various numbers of membrane-associated particles (MAP) (Fig. 2). At the nexus, oval or bizarre-shaped patches or macules studded with small particles were seen on the fractured membranes (Figs. 2, 3). The *en face* view of the cytomembrane showed undulation. For example, in Fig. 3 an extensive waving as well as mild rippling are clearly visualized.

Nexus (gap junction)

The configuration of the nexus was variable; it consisted of round to oval macules with great variation, ranging from 0.2 to 0.6 μm in long diameter (Figs. 3, 4). Individual macules could coalesce to form large, bizarre-shaped ones. The nexus could extend to a large area and islands of non-nexus areas could be entirely enclosed (Fig. 3, inset). Particulate aggregates elevated to various heights above the plane of fracture (Figs. 3, 4) and less frequently, similarly arranged pits (Fig. 4, inset) were clearly seen. In some areas particles were arranged in lattices of variable regularity (Fig. 3). Orderly register of particles was better recognized in a low magnification (Fig. 3). The number of MAP was variable, depending on the specimen (Fig. 2 vs. Figs. 3, 4). In general, MAPs were not as many as previously reported (9, 10), even on the A-face of many specimens.

Face-A at nexus

Since in many preparations MAPs were not abundant on the A face, and the B face did not show many pits but mostly a "cobblestone" pattern, the only criterion to distinguish the A face from the B face was an abundance of high particles at the nexus that were rather regularly elevated from the plane of fracture (Figs. 4, 5*a*). Although the B face had a fair number of particles, their number was usually less than 1/3 of the cobblestones and their height varied markedly (Figs. 4, 5*a*, 6*a*).

The typical face-A particle at the nexus had a long diameter of 100–135 Å and a height of 50–70 Å. They were round or polygonal. In many nexuses, aggregation of face-A particles was partially covered with face-B cobblestone particles of the apposed keratinocyte membrane (Figs. 4, 5*a*). Face-A particles were individually similar to scattered MAPs which measured about 100 Å in diameter (Figs. 2, 4, 5*a*).

Face-B at nexus

Face-B surface, particularly that of the finger skin obtained from the roof of a friction blister, showed very few MAP (Figs. 4, 5*a*, 6*a*). Nexus macules on the B Face were usually very well demarcated and either slightly depressed (Fig. 2), level with Lm2, or slightly elevated (Fig. 4). The macule was studded with low and high particles. Low particles outnumbered the high particles. The high particles appeared very similar in size (100–135 Å), height (50–70 Å), and configuration to those on the A surface (Figs. 4, 5*a*). The low particles were round, oval or polygonal, i.e., square to hexagonal, and showed a great variation of size, ranging from 70 Å to 135 Å (Figs. 4, 5*a*, 6*a*). Their height also varied from almost level with the fracture surface, up to 25 Å. Crater-like central depressions, measuring about 25–40 Å, were seen in some particles. Those low particles were compatible with the "cobblestone-type" B face nexus structures, as mentioned by McNutt & Weinstein (9). When shadowed at a high angle, pits, measuring 45–50 Å, were occasionally observed (Fig. 4, inset). Lm2, which carries the B surface, often showed a serrated edge in non-nexus areas (Fig. 4, inset), suggesting that Lm2 is composed of globular subunits.

Tight junctions

No tight junctions were found in this study. If present, they should have been recognized as ridges and grooves juxtaposed to the nexus [7]. It is obvious that the lateral tight junction of the stratum granulosum of the normal skin [7] was not fractured in this study.

Desmosomes

Specialized areas on the B face as shown by McNutt et al. (10) were occasionally observed in the fixed specimens. They consisted of a clustering of small

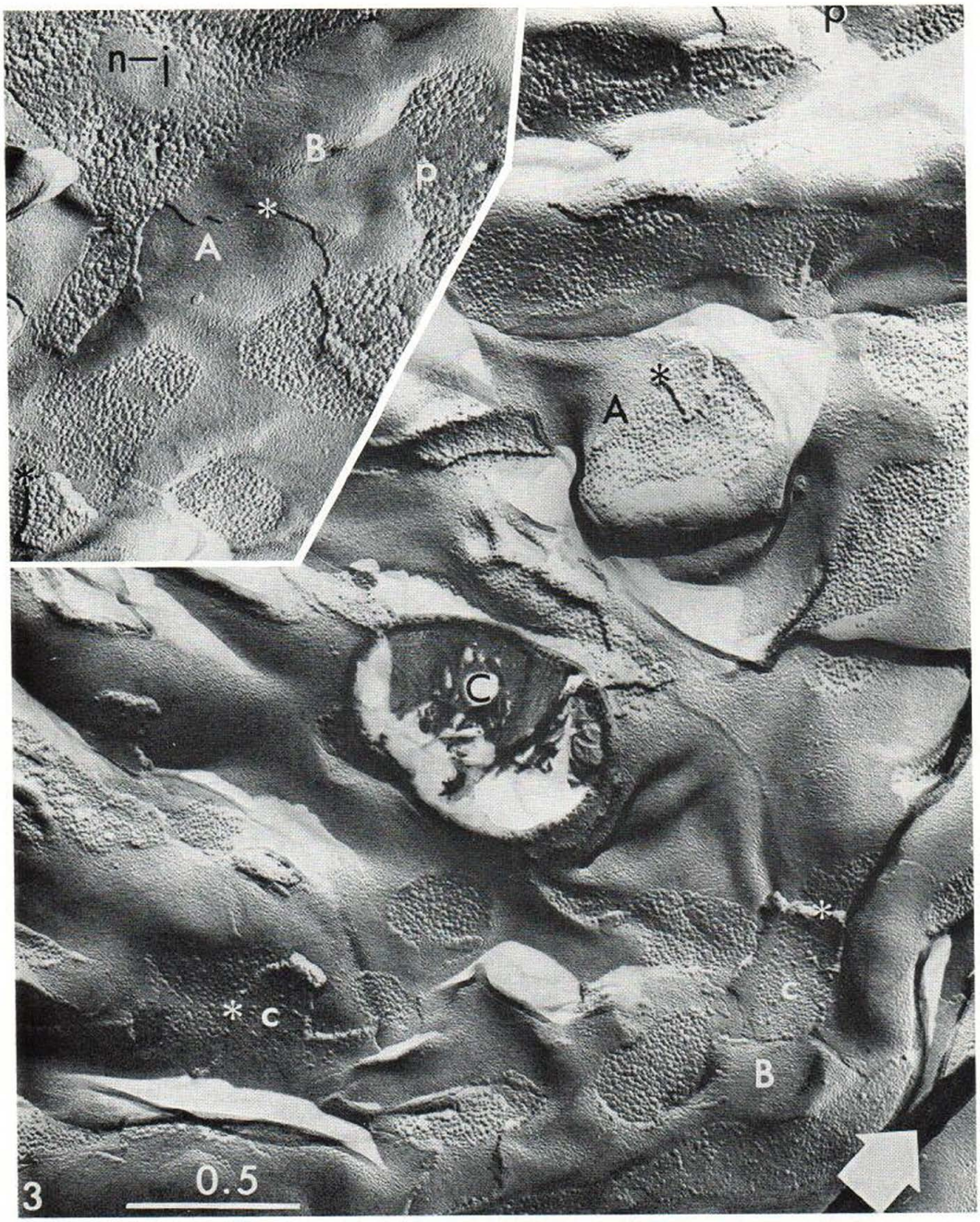

Fig. 3. A large area of the fractured membrane surface of the basal cells exhibits extensive indulation. In one area, the dermal collagen is seen (*C*). The fracture revealed both A- and B-faces. At nexuses, the A-face (*A*) shows a cluster of contact cylinders in well-defined macules occasionally in register, whereas the B-face (*B*) shows either cobblestone-like low particles (*c*) or pits (*p*). In many nexuses, Lm2 with B-face cobblestones is partially peeled off (*) and Lm1s of the apposed cell with A-face contact cylinders are revealed. Finger skin. × 50 000. *Inset:* two large nexuses, probably formed by confluence of smaller ones. Non-junctional B-face (*n–j*) is enclosed within one of them. Other labels are the same as in the main figure. Finger skin, × 50 000.

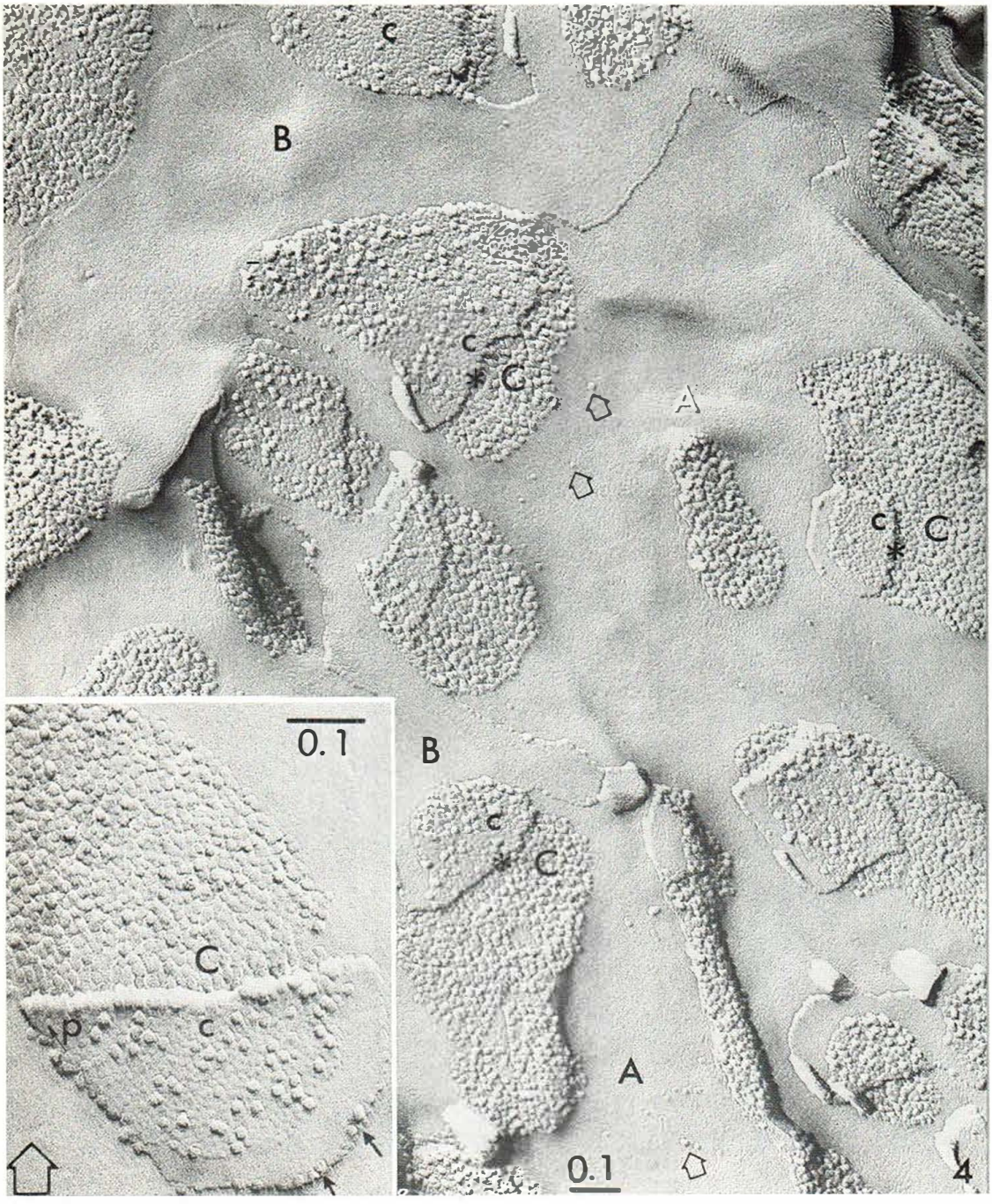

Fig. 4. A higher magnification of face A and face B. Face A (*A*) has some scattered MAPs (small hollow arrows) and clustered contact cylinder particles (*C*), whereas, face B (*B*) is smooth with few MAPs and has cobblestone particles (*c*) admixed with high particles similar to face A contact cylinders. A good correspondence of configuration of nexuses between face A and face B can be seen where face B is partially lifted (*). It must be mentioned here that between the cobblestone membrane, i.e., Lm2, and the membrane on which A-face particles are situated, i.e., Lm1, there is a tightly apposed intercellular space of nexus (at *) and that Lm2 and Lm1 belong to different cells (see Fig. 1*a*). Lm2 shows globular subunits even in non-nexus areas (thin, solid arrow in the inset) and often reveals a serrated edge. Finger skin, × 75 000. *Inset:* finger skin, × 112 500.

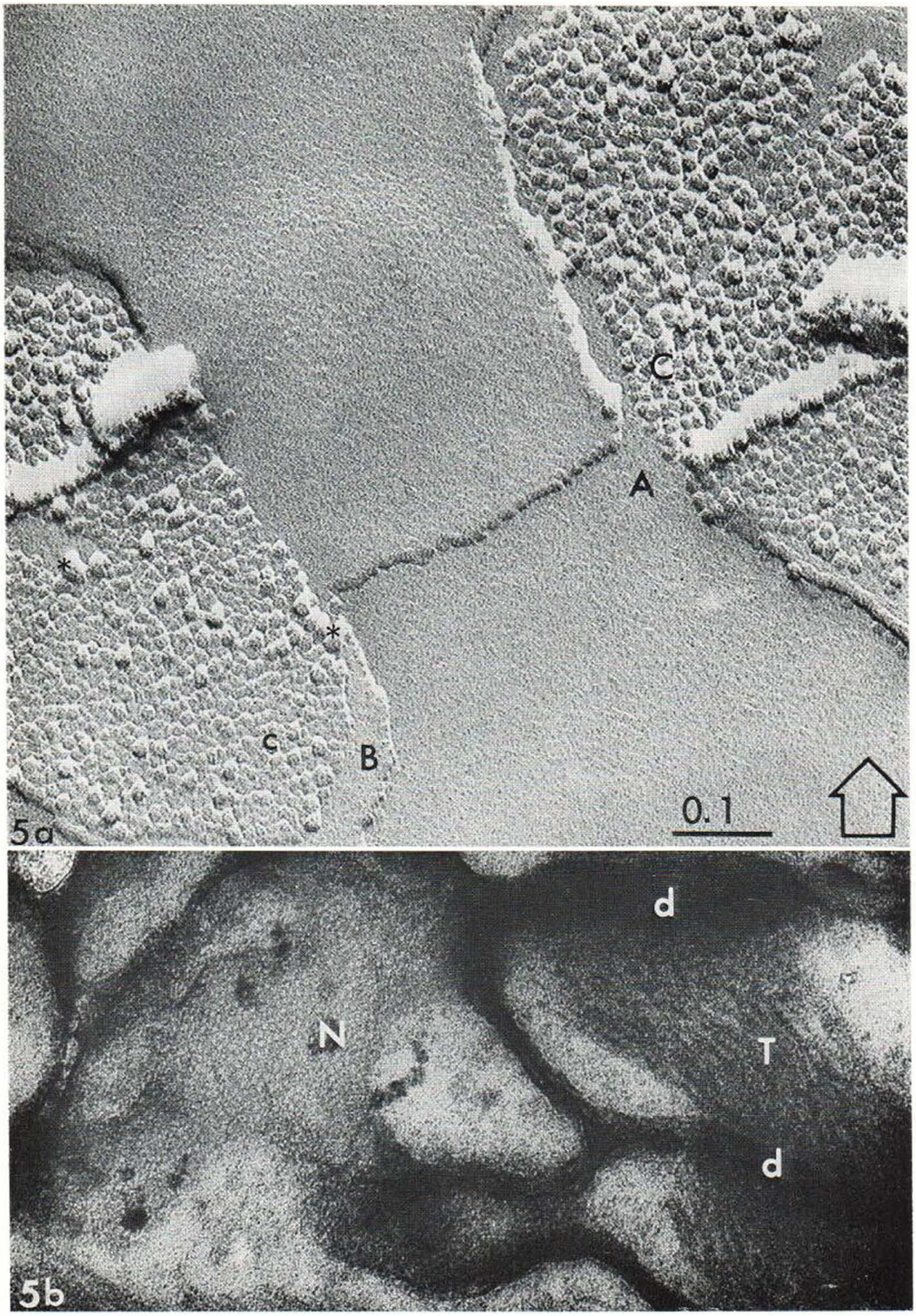

Fig. 5. (*a*) A still higher magnification of the A-face (*A*) showing contact cylinders (*C*), with dimensions of 100–135 Å in diameter and 50–70 Å in height. The B-face (*b*) has mainly cobblestone-type particles (*c*), 70–135 Å in diameter and 0–25 Å in height, but higher particles (*) similar to contact cylinders are also admixed. Finger skin, × 150 000.

(*b*) Lanthanum-permeated skin of the arm shows lanthanum-filled intercellular spaces. Nexus (*N*) which follows desmosome (*d*) shows small, unstained particles measuring about 70 Å. *T*, tonofibrils. × 150 000.

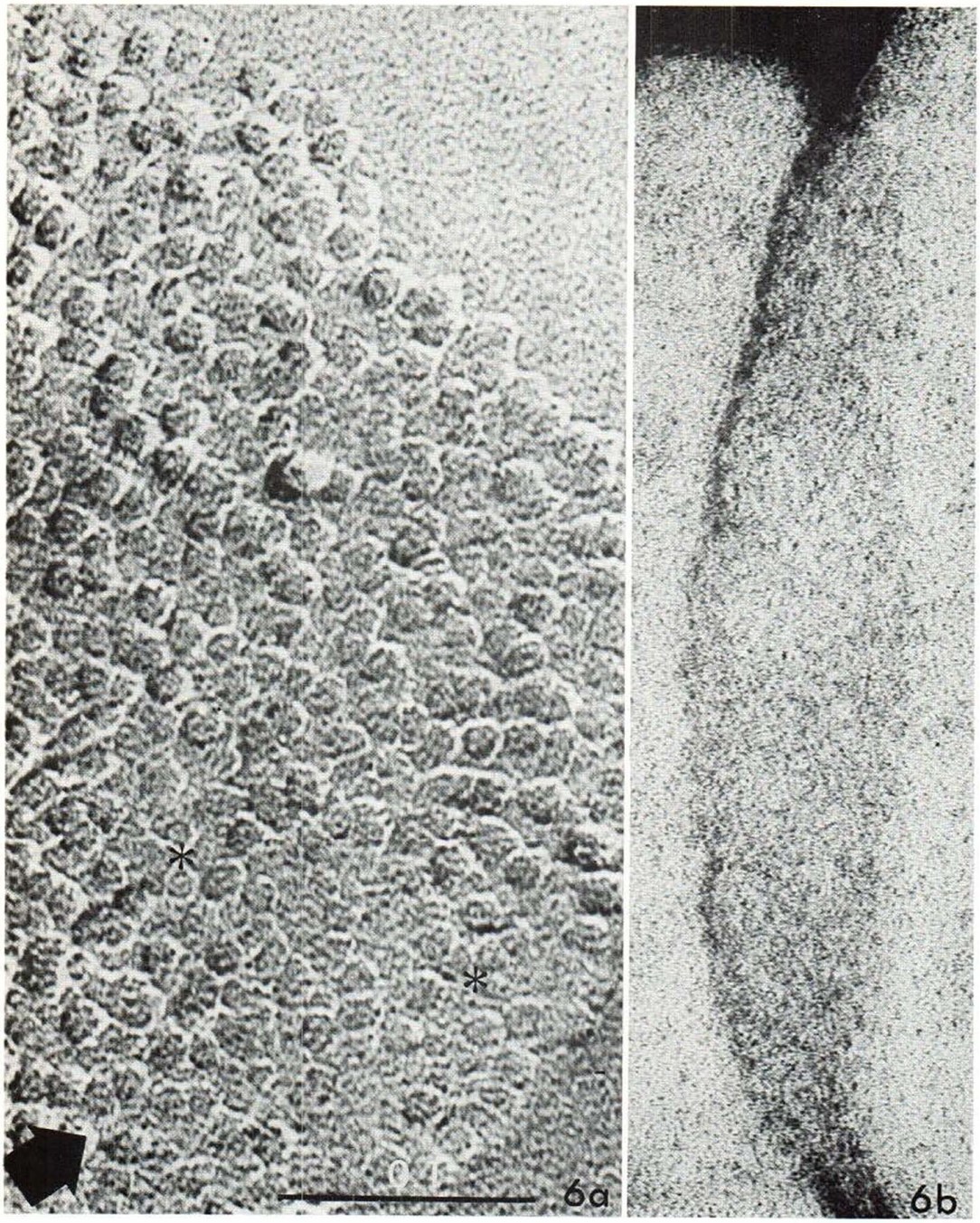

Fig. 6. (*a*) A very high magnification of cobblestone particles revealed the round to polygonal contour of individual particles measuring 70–135 Å in diameter. If the correction factor of 2/3 were applied, (1, 14), the actual sizes of these particles would be 45–90 Å. It is possible that some of the low particles (*) were not fully shadowed and, therefore, appear smaller than actual size. Finger skin. × 375 000.

(*b*) Lanthanum-permeated skin of the arm shows non-stained nexus subunits which measure about 70–75 Å. × 375 000.

particles within an ill-defined area between the nexuses (Fig. 2, inset). In the human epidermis the nexuses generally exist juxtaposed to desmosomes [7] (see below).

Nexus subunits in thin sections

The nexus was usually present very closely juxtaposed to desmosomes (Fig. 5*b*). Without lanthanum it was seen clearly only in cross section as 20–30 Å slits with a central dense layer sandwiched between two cytomembranes of apposed cells. The sizes of the nexus were varied greatly, but usually ranged between 0.1 and 0.6 μm in diameter, thus agreeing in size with nexus macules that were demonstrated in the replica. Lanthanum permeated the intercellular spaces and infiltrated 20–30 Å nexus gaps which in lateral view showed small subunits (Figs. 5*b*, 6*b*). Lanthanum filled the narrow channels between subunits, but subunits themselves were not stained. The subunits were round to polygonal with a diameter of 70–75 Å (Figs. 5*b*, 6*b*).

DISCUSSION

Cell surface ultrastructure of freeze-cleaved keratinocytes of the epidermis is not expected to differ greatly from that of the normal cervical epithelium. Nevertheless, our observations are at some variance with those of McNutt & Weinstein (9) and McNutt et al. (10). Regrettably, only one replica electron micrograph at a low magnification was included in their publication (10) and the information extractable therefrom is certainly limited. Since they did not specifically mention in the caption whether the specimen was derived from a keratinizing part of the cervix uteri, comparison with the skin is difficult. In my preparation, the majority of B face structures at the nexus showed a cobblestone pattern instead of pits. Although they did not publish the cobblestone pictures, McNutt & Weinstein (9) gave their dimensions: 90–100 Å in diameter and a height of 35 Å in the replica. The cobblestones of the epidermal keratinocytes, as shown in Figs. 5*a* and 6*a*, were found to be more variable in diameter (70–135 Å) and height (0–25 Å). Also, a variable number of high particles similar to face A particles at nexus (contact cylinder) were admixed. These high particles might actually represent the contact cylinders which happened to be tightly engaged in pits of Lm2 on the B surface and, when fractured, were pulled out from the A surface side of Lm1 where, according to McNutt & Weinstein (9), they are supposed to stay (Figs. 1*a*, 1*b*): In the other tissues and cells or with other techniques (2, 4, 9, 10), the contact cylinders of nexus seem to go with Lm1 and project from the A face. A possibility that a deep etching produced high particles was considered. However, in the same B face the majority of cobblestones remained low, suggesting that there was a definite difference of height among these particles at the time of membrane fracture.

It is certain that cobblestones are present on the same plane and in the same area as B face pits are situated, since the pits and cobblestones are simultaneously demonstrated within the same nexus (Fig. 4, inset). As mentioned by McNutt & Weinstein (9), where the B face was shadowed at a high angle and hence platinum was deposited densely, pits were seen (Fig. 4, inset).

In the same nexus where the B face was shadowed at a low angle and hence the deposition of platinum was light, a cobblestone pattern was revealed (Fig. 4, inset). There is no explanation, however, of why the low angle shadow-casting produces cobblestone patterns. A puzzling problem is that even a high angle-shadowed B face did not necessarily show pits, but showed the cobblestone pattern instead (Fig. 3). It may then be postulated that upon cleavage the contact cylinders can be (i) pulled out of the B face, leaving typical pits, (ii) broken at various levels above the B face plane up to 25 Å, or (iii) left with the B face as "high particles". In fact, the height of contact cylinders on the A face is not uniform in some nexuses (Fig. 5*a*); the short ones could represent the complementary half of high B face particles. In the nexus of keratinocytes, the second and third possibilities might actually occur (Figs. 1*a*, 1*b*), or it is possible that this is due to the difference of technique used in the present study. This problem may be solved by making double replicas and examining the complementary set of fractured surfaces.

Slight variations from the previously published data (9, 10) were noted in calculated dimensions of some structures such as the diameter of contact cylinders (Table I). Several technical factors involved in this method may distort the true dimensions: the angle of shadowing, thickness of the replica, deformation of the fractured surface prior to replication (fluctuation of ambient temperature, etc.), etching by sublimation, and contamination of vacuum. The noted variations are very likely due to these uncon-

Table I. *Measurement of nexus subunit in replica and in thin section*

	A-face particle (contact cylinder)		B-face pit		B-face cobblestone		Nexus subunits (with La stain)	
	Diameter (Å)	Height (Å)	Diameter (Å)	Height	Diameter (Å)	Height (Å)	Diameter (Å)	Height (Å)
McNutt & Weinstein (9)	50–75	50	30–50		90–100	35		
Revel & Karnowsky (13)							70–75	50
Goodenough & Revel (4)	90–100		<90–100[a]				90–100[a]	
Hashimoto (present study)	100–135	50–70	45–50		70–135	0–25	70–75	

[a] Center-to-center measurement.

trollable factors in each investigator's method, and probably not due to a specific difference of the tissue examined.

If an approximate correction factor of 2/3 (8) can be applied to replica dimensions to reduce the actual sizes of structures that are copied on replica, contact cylinders should measure between 65–90 Å and cobblestones between 45–90 Å. The lanthanum-delineated nexus subunits pictured in the same microscope at the same accelerating voltage measured 70–75 Å in diameter. If the reduction of size, due to fixation, dehydration, and lipid extraction by alcohol and propylene oxide is considered, the actual sizes of these subunits could be greater than 70–75 Å. If 20% reduction is a reasonable figure, they should measure approximately 85–90 Å in vivo. Thus, both contact cylinders and cobblestone particles seem to be smaller than these subunits. According to McNutt & Weinstein (9), the nexus subunits may represent the caps covering the contact cylinders on the D face of Lm2 (Figs. 1*a*, 1*b*).

In this study, not many specific structures were noted which might correspond to desmosomes. McNutt et al. (10) described an accumulation of small particles as an imprint of a desmosome on the B face in cervical epithelium. In many replicas, careful examination was made in the areas between nexuses where desmosomes are expected to occur in the epidermis (7). Such areas were found to be more often than not smooth on both A and B surfaces. Since MAPs were still demonstrated in these areas (Fig. 4), the possibility that a heavy casting of metal buried desmosomal particles could be ruled out. It may be tentatively stated that, with the present method, desmosomal marks on fractured membranes can be detected only occasionally in the human epidermis.

Acta Dermatovener (Stockholm) 54

ACKNOWLEDGEMENT

This work was supported by a Medical Investigatorship Award and a Designated Research Grant from the Veterans Aministration.

REFERENCES

1. Branton, D.: Fracture faces of frozen membranes. Proc Nat Acad Sci (USA) *55:* 1048, 1966.
2. Chalcroft, J. P. & Bullivant, S.: An interpretation of liver cell membrane and junction structure based on observation of freeze-fracture replicas of both sides of the fracture. J Cell Biol *47:* 49, 1970.
3. Deamer, D. W. & Branton, D.: Fracture planes in an ice-bilayer model membrane system. Sci *158:* 655, 1967.
4. Goodenough, D. A. & Revel, J. P.: A fine structural analysis of intercellular junctions in the mouse liver. J Cell Biol *45:* 272, 1970.
5. Hashimoto, K.: Demonstration of the intercellular spaces of the human eccrine sweat gland by lanthanum. I. The secretory coil. J Ultrastruct Res *36:* 249, 1971.
6. — Demonstration of the intercellular spaces of the human eccrine sweat gland by lanthanum. II. The duct. J Ultrastruct Res *37:* 504, 1971.
7. — Intercellular spaces of the human epidermis as demonstrated with lanthanum. J Invest Dermatol *57:* 17, 1971.
8. Lessin, L. S., Jensen, W. J. & Ponder, E.: Molecular mechanism of hemolytic anemia in homozygous hemoglobin C disease. J Exp Med *130:* 443, 1969.
9. McNutt, N. S. & Weinstein, R. S.: The ultrastructure of the nexus. J Cell Biol *47:* 666, 1970.
10. McNutt, N. S., Hershberg, R. A. & Weinstein, R. S.: Further observations on the occurrence of nexuses in benign and malignant human cervical epithelium. J Cell Biol *51:* 805, 1971.
11. Muhlethaler, K., Moor, H. & Szarkowski, J. W.: The ultrastructure of the chloroplast lamellae (Spinacea oleracea). Planta *67:* 305, 1965.
12. Pinto da Silva, P. & Branton, D.: Membrane splitting in freeze-etching. J Cell Biol *45:* 598, 1970.
13. Revel, J. P. & Karnowsky, M. P.: Hexagonal array of subunits in intercellular junctions of the mouse heart and liver. J Cell Biol *33:* c7, 1967.

14. Staehelin, L. A.: The interpretation of freeze-etched artificial and biological membranes. J Ultrastruct Res *22:* 326, 1968.
15. Tillack, T. W. & Marchesi, V. T.: Demonstration of the outer surface of freeze-etched red blood cell membranes. J Cell Biol *45:* 649, 1970.

Received August 28, 1973

K. Hashimoto, M.D.
Veterans Administration Hospital
1030 Jefferson Avenue
Memphis, Tennessee 38104
USA

ADDENDUM

After completion of this manuscript, Breathnach et al. (Micron *3*: 287, 1972; J Anat *114*: 65, 1973) described aggregations of small particles found on freeze-fractured human epidermal cell membranes as desmosomal particles. These clustered particles were seen on elevated areas of fractured membrane which is directed toward the cytoplasm. No complementary structures were found at lower levels, but in stratum corneum similar aggregations were seen on slightly depressed areas of outwardly directed fracture surface.